Spatial organisation of catchments - assessment and usage for impartial sub-basin ascertainment and classification

Henning Oppel[1], Andreas Schumann[1]

[1]Institute of Hydrology, Water Resources Management and Environmental Engineering, Ruhr-University Bochum, Bochum, 44801, Germany

Correspondence to: Henning Oppel (henning.oppel@rub.de)

Abstract.

A hydrological model should represent the hydrological most relevant catchment characteristics. These are heterogeneously distributed within a watershed but often interrelated and subject of a certain spatial organisation. In order to reproduce the natural rainfall-runoff response the reduction of variance of catchment properties as well as the incorporation of the spatial organisation of the catchment is desirable. In this study the method of the characteristic structure is introduced to detect and visualize the spatial organisation of catchments, based on stream flow length rearrangement of any catchment feature of interest. Moreover, the method is implemented in an algorithm for automated sub-basin ascertainment, which includes the definition of zones within the newly defined sub-basins. The algorithm is applied on two parameters characterising topography and soil of four mid-European watersheds. Results indicate a wide range of applicability for the method and the algorithm. As a limitation of the application for the algorithm the presence of small scale soil enclosures that do not follow the geomorphologic structure of the catchment could be identified. Finally, results of subdivisions based on soil and topography were intersected to gain insight into catchment organisation. Based on this analysis four physiographical types of different sub-basin spatial organisations could be established.

1 Introduction

The identification of landscape units featuring an identical, or at least similar, hydrologic behaviour is a prevailing topic in hydrology. A valid and widely applicable concept is essential by two reasons: for the use in rainfall-runoff-models and the use in regionalization concepts concerning the prediction in ungauged basins (Sivapalan et al., 2003). Within rainfall-runoff-models these spatial units could define parameter constraints for distributed and semi-distributed models and could, hence, lower the problem of equifinality (Beven, 2006). On the other hand it would enable a profound method for information transfer from gauged to ungauged basins, or could be used as non-Euclidian distance measure to specify the degree of similarity of two catchments (Skøien et al., 2006).

How these units can be identified is, despite all scientific effort, still unresolved. There are several concepts and findings in the scientific literature. The common foundation for all concepts is the interaction of the physiographic and the hydrological

system within a basin. Winter (2001) expressed that this interaction forms hydrological landscapes, which are defined by landscape, geological framework, climate, surface-, ground- and atmospheric water. The analysis of the hydrologic system is bound to discharge time-series analysis (beside the special case of experimental watersheds) and several catchment classification schemes have been established to identify basins of similar hydrological behaviour (He et al., 2011; Merz and Blöschl, 2003; Sawicz et al., 2011; Wagener et al., 2007). Contrary to analysis of the hydrologic system where the crucial variable (discharge) is known, the variable(s), yet the number of variables causing the characteristic hydrological behaviour are mostly unknown. This makes the analysis of the physiographic system (the interplay of topography, soil land cover, etc.) more complex than the analysis of the hydrologic system. Studies have shown that catchments with similar soil and topographical values are featuring similar rainfall-runoff dynamics (Müller et al., 2009; Güntner et al., 2004) and therefore most classification schemes try to combine these features (Müller et al., 2009; Dunn and Lilly, 2001; Soulsby et al., 2006). However, these strategies are mostly restricted to a single characteristic. Sivapalan (2005) pointed out that the organisation of a catchment is the fundamental influence on the hydrologic system. Patterns of symmetry between soil, topography and the stream network could give insight to underlying mechanisms that induce discharge behaviour. Well known methods to assess the organisation are mainly based on the stream network (Rodríguez-Iturbe and Valdés, 1979; Verdin and Verdin, 1999; Skøien et al., 2006). But these methods neglect information about interdependencies between soil and topography of the catchment. The heights above the nearest drainage concept and classification scheme by Nobre et al. (2011) Gharari et al. (2011) and Savenije (2010) takes the geomorphologic allocation of basins cells into account and defines hydrological response units (HRU). This concept does account for soil, topography and their interaction but omits the exact location and possible interactions along the flow path within a basin.

In this study we will present a method for automated sub-basin ascertainment based on the spatial organisation of a watershed. First we will introduce the required basic theories and techniques for such a method. A flow path orientated tool for the assessment of spatial organisation of catchments, called the method of characteristic structures will be introduced in this part of the paper. Afterwards this method will be incorporated into an algorithm to perform a subdivision of a catchment based on its individual spatial organisation. The proposed methods are based on a flow path orientated rearrangement of catchment characteristics. With the connection to the flow path this analysis brings insight to processes of lateral flow distribution (Grayson and Blöschl, 2001). In contrast to classic methods for spatial pattern evaluation (like Point-by-Point or optimal logical alignment methods (Grayson and Blöschl, 2001)) the new method retains information about location and position in the succession of catchment characteristics along the flow path axis.

After the outline of the basic theory in Sec. 2 we address the general applicability of the proposed method. Therefore the algorithm was applied to soil and topography characteristics of four meso-scale mid-European watersheds. Based on this results we will evaluate the performance of the algorithm and examine if boundaries for its application are in evidence. In course of this assessment a numerical experiment was carried out to examine different catchment structures with an identical range of values (topography and soil). Results of the application are presented in Sec. 3 and the discussion can be found in Sec. 4.

Beside its general applicability its value for different hydrological applications is addressed. On the one hand we compare automatically ascertained sub-basins to sub-basins defined by a common approach. On the other hand we give a prospect to the use in regionalisation and catchment classification topics. Based on spatial patterns visible in the outcome of the algorithm we established a threshold-based classification scheme to identify different physiographical types.

With this concept of the paper we tend to introduce our methods, proof its applicability and give references to possible hydrological applications. The final conclusion and a summary of the obtained results will be given in Sec. 5.

2 Methods and Data

The following sections intend to present data, catchments and methods used in this study. First subsection will describe the data. Afterwards a newly developed method for the assessment of spatial organisation of catchments will be introduced. Finally a brief introduction to the implementation of the beforehand proposed methods into an algorithm for automated sub-basin ascertainment will be given.

2.1 Data

Four catchments were chosen for application. The basin of the Mulde (Fig. 1, lower right) is located mostly in eastern Germany and with a small part in north Czech. It covers the mid-range mountainous region of the Ore Mountains in the south and the Mulde Loess Loam Hills in the north. With a size of 6170 km^2 it is the largest catchment used in this study. Located in the Bohemain Forest in west Bavaria, the catchment of the river Regen (Fig. 1 upper left) is with a size of 2613 km^2 the smallest river basin used for application. The headwater catchment of the Main (Fig. 1, upper right), including the White and Red Main comprises an area of 4224 km^2. Last selected catchment is an alpine catchment with similar size to the Mulde, the catchment of the Salzach in Salzburg, Austria, comprising an area of 5995 km^2. All catchment own different geomorphologic structures and river network types. While in the first three catchments, higher mountains are nearly exclusively located at the outer watershed of the catchment, the Salzach catchments contains three big mountains located at the centre of the catchment. The two main tributaries encompass these mountains. While the basin of the Mulde has a nearly continuous increase of slope and heights from north to south, the topography of the remaining catchments is much more heterogeneous.

For the proposed methods and algorithm at least a digital elevation model (DEM) is essential. For this study we used a gridded DEM derived from the Shuttle Radar Topography Mission (SRTM) with a regular 100 meter resolution. By means of the D8-algorithm the required data like flow directions, flow length and flow accumulation were calculated (Jenson and Domingue, 1988). For the catchment of the Mulde a proved digital river network was available. Stream networks of the remaining basins were calculated via flow accumulation algorithms. Because it is envisaged to subdivide the presented catchments by soil characteristics, a gridded soil data map by the German Federal Institute for Geosciences and Natural Resources (BÜK200) and CORINE land coverage data (CLC) (Bossard et al., 2000) were used. Pedo-transfer functions (Sponagel, 2005) combined these information into gridded data about (available) water capacities, hydraulic conductivities and other characteristics. In case of

the Salzach basin precast pore volume data for the LARSIM-ME model were used, due to a lack of soil data (Bremicker, 2016). The used soil and topography input data comprises a certain amount of uncertainty, due to the fact that they are derived data. The uncertainty of the input data is neglected in the performed case studies. Pore volume data is depicted in Fig. 2 for watersheds of the Main, Regen and Salzach. Data for the Mulde basin is shown in Fig. 3. Beside the mentioned topographical structure of the basin we can now see similarities and differences in the pedologic system. The dependency of pore volume and elevation is common for all basins, mountainous regions tend to have lower values than flat lands. A main difference is the arrangement of higher values. While in the Salzach catchment only mid-range values align around the streams and only smaller spots of higher values are present, the catchment of the Mulde has a break between high and low values in the middle of the basin. Moreover, wide soil belts with high pore volume encompass the river valleys in transition area. In comparison to these pattern, soils in the Regen and Main basin seem nearly homogenous with respect to some stripes of higher values near the outlet of the basins. Please note that the basin of the Mulde is our development basin. Parameters and thresholds used in the case study are derived from this basin. The remaining basins are used for validation of the proposed method.

2.2 The method of characteristic structures

River discharge is the result of interactions between atmospheric inputs and the landscape. This interaction can be interpreted as the way water moves vertically and horizontally through the watershed towards the outlet. Differences between catchments, not arising from different atmospheric inputs, are therefore result of different flow path characteristics. If we consider a specific catchment characteristic, like soil or topography, the succession of these values along the flow path within the catchment can be interpreted as the organisation of the watershed.

Flow paths can be detected by means of a DEM and the D8-algorithm (Jenson and Domingue, 1988) and are quantified as length to the drainage. In this study the flow length are differentiated by their surrounding medium. Lateral flow lengths are divided into flow lengths within the river network to the outlet (called stream flow length (SFL)) and along the land surface to the next stream cell (defined as over land flow length (OFL)). Note that the perspective is set upstream.

In order to characterise the succession of soil, topography or other characteristics we have to assign these values to each point of the flow path. In a catchment where each flow length is unique all occurring values of the catchment characteristic of interest can be used as the description directly. Since this is not the case in natural catchments, where multiple parallel streams and hillslopes are present, all equidistant points within the catchment have to be drawn together. With the use of average values and standard deviation (one-sigma range) of equidistant points the succession of catchment characteristics along the flow path can be assessed. Results of the described procedure will be addressed as a “characteristic structure”. As an example Fig. 3 shows the map of available water capacity (AWC) in the Mulde catchment and its characteristic structure.

Averages and the one-sigma range of standard deviations are plotted as continuous lines, yet underlying data is point wise. Caused by the non-continuous solution (consequence of gridded data and depending on grid size) of distance data. For compensation distances are ordered into classes. Parameter Δs for SFL- and Δo for OFL length are width-thresholds utilised to define distance classes. The basin is thereafter treated as succession of SFL- and OFL-classes. All grid cells of the catchment

are merged in their respective distance-class (for the presented catchments a value for Δs in a range from 1 to 10 km proved to be most adequate). Within each SFL-class an average value and the standard deviation of the characteristic of interest can be calculated:

$$\bar{X}_{sfl} = \frac{1}{n_{Cells;sfl}} \sum_{j=0}^{n_{Cells;sfl}} X_j \quad (1)$$

$$\sigma_{sfl} = \sqrt{\frac{1}{n_{Cells;sfl} - 1} \sum_{j=1}^{n_{Cells;sfl}} \left(X_j - \bar{X}_j \right)^2} \quad (2)$$

where sfl indicates the SFL-class, $n_{Cells,sfl}$ is the number of cells assigned to this class and X is the characteristic of interest. If the average and the standard deviation of each class is plotted against its average distance to the outlet, the characteristic structure of the catchments is made visible (as shown in Fig. 3).

An extension of this method is to take the OFL-classes into account additionally. By their distance to the next stream it is possible to distinguish between regions which are close to stream or more distant and to evaluate the catchment characteristic for these regions separately. In Fig. 4 the characteristic structure of AWC is separated by distance classes of OFL (width of Δo = 100m). Instead of the one-σ-range, averages of OFL-classes are depicted. From these analysis one might conclude that the variance in the SFL classes (in Fig.3) is mainly caused by differences of AWC according to the distance from stream cells.

Note that the method can be applied to all gridded data with a metric scale (soil, climate, topography, etc.). Moreover, it is possible to identify shifts of means and variance along the flow path and can allocate their placement within the catchment.

2.3 An algorithm for automated sub-basin ascertainment

The example characteristic structure in Fig. 3 exhibits that in some parts of the basin equidistant regions comprise similar AWC-values and, hence, the standard deviation is low. In other regions, especially in the centre of the basin, the equidistant regions are very heterogeneous and comprise high standard deviation.

For most hydrological purposes (modelling, regionalisation, search for hydrological units, etc.) homogenous sub-basins are essentially required. Therefore it seems likely to use the proposed method to identify the need for division of a catchment into sub-basin.

For the extension of the method of characteristic structures into an algorithm for sub-basin ascertainment several functionalities have to be introduced:

1. An Objective function to identify the need and position of necessary subdivisions.
2. A Subdivision tools for the actual partition of the catchment.
3. An evaluation strategy for performed subdivisions.

The following subsections will give a brief introduction to these three functionalities, afterwards the sequence of the final algorithm will be described. For more details about the introduced tools please see Appendix A.

2.3.1 Objective Function

The value of the objective function is calculated from the characteristic structure of the standard deviation σ, shown in Fig. 5. A casual observer will easily spot regions with higher σ that should be considered for ascertainment. To make this feasible for the algorithm a threshold value Ω has been introduced that states whether a SFL-class is to categorise as "low" or as "high" variance class. Threshold Ω is derived from the data by:

$$\Omega = \frac{\sum_{j=0}^{N_{sfl}} \omega_j^{\,e} \cdot \sigma_j}{\sum_{j=0}^{N_{sfl}} \omega_j} \tag{3}$$

where N_{sfl} is the number of SFL-classes, σ is the standard deviation within SFL-class j (Eq. (2)), the exponent e is a variable non-linearity factor and ω a weighting factor is defined as:

$$\omega_j = \frac{\sigma_j - \max_{sfl}(\sigma)}{\min_{sfl}(\sigma) - \max_{sfl}(\sigma)} \tag{4}$$

As index N_{SFL} in Eq. (3) indicates threshold Ω is calculated for the entire catchment and does not necessarily represent the true value of σ for "homogeneous" sub-basins/SFL-classes. It only delimits between present high and low variance. Dependent on the purpose it might be advisable to recursively apply the proposed algorithm for further reduction of Ω and hence the remaining variance. Note that each application will lead to a higher number of subdivisions.

Coherent SFL-classes above the threshold are considered as high variance *regions* within the basin that require spatial separation. If regions of SFL-classes below the threshold are found, these regions will be marked as low variance regions.

2.3.2 Subdivision tools

Figure 6 introduces a synthetic catchment, its stream network, distance classes and a sample catchment characteristic which can be used as input data (for the algorithm under development). The application of the objective function has three possible outcomes:

1. All SFL-classes are below threshold Ω,
2. Parts of the SFL-classes are below Ω,
3. No SFL-classes are below Ω.

First case indicates that no subdivision is required. Consequently no tool has to be applied. Second case indicates that a coherent part of the flow path comprise homogenous characteristics. This case is depicted in the upper left part of Fig. 7. Hatched cells indicate the low variance region. Since this region is homogenous it will not require any further handling and should be clipped from the rest of the basin.

The first developed tool is called *Separation*, since its task is to separate low variance regions from high variance regions. To comply with its task the tool searches the ideal drainage points to capture a maximum of the low variance regions. The search for these separation points is made iteratively close to the transition from low variance SFL- to high variance SFL-classes. In the upper middle of Fig. 7 the result of *Separation* is shown for the introduced synthetic catchment. Black dots indicate the identified drainage points, hollow points indicate rejected points. After applying the *Separation* tool, three sub-basins were defined. One containing the low variance regions that do not require any further treatment and the other two sub-basins comprising the remaining parts of the catchment.

These heterogeneous sub-basins will most likely be subject to the third part of the structuring procedure. In this case all SFL-classes are coherently above the threshold. High variance of catchment characteristics within a watershed can arise from different sources. On the one hand, parallel streams or more specifically neighbouring valleys with different vegetation, slope, etc. will cause high variance in the characteristic structure of the entire basin. On the other hand wetlands close to stream often expose different characteristics as the contributing hillslopes. These patterns are a result of the co-evolutional formation of catchments (Blöschl et al., 2013; Sivapalan, 2005). These stream network orientated patterns for pore volume are visible e. g. in Fig. 2 and Fig. 3.

To account for these two origins of heterogeneity, two tools were developed. The first tool is *Subdivision at ramification* which defines new sub-basins at confluences, or ramifications points because our perspective is upstream, of higher order streams. The second tool is a *zonal classification* scheme. Cells within a basin are separated by their distance to their draining stream cell and the respective Strahler order. Distance and order are defined iteratively and obtained zones are called "close to stream -" and "far from stream zones" dependent on their distance to the stream. In the lower part of Fig. 7 both tools are applied to the exemplary synthetic catchment. Hatched cells in the lower left depiction are high variance regions that require partition. Results of the *Subdivision at ramification* tool gives two additional drainage points and basins, results of the *zonal classification* gives no new drainage points but rather two zones belonging to the beforehand defined drainage points.

2.3.3 Evaluation

If one beforehand introduced tools has been applied to lower the standard deviation σ in the watershed, it has to be evaluated if this target has been achieved. Therefore we have to reinterpret the objective function. The objective function has been defined to minimise the deviation of a catchment characteristic σ within each distance class. A tool is activated if σ is above threshold Ω. After its application two, or more, parallel basins are present in the same distance class. Note that the distance classes are associated to the flow path within the entire catchment. By introducing these parallel basins we intend to merge similar values and therefore try to lower the average deviation within the distance class. This evaluation technique can be expressed as follows: Let B be the number the sub-basins defined within an original watershed U. First step is to calculate the standard deviation σ (Eq. 2) within each sub-basin with SFL-classes based on flow length within the sub-basins.

In the second step the calculated σ-Values are transferred to the flow-length axis of the original watershed O. This is done for all sub-basins. Finally the new standard deviation σ(S) for the separated basin is calculated for each SFL-class as average of all σ values assigned to the same SFL-class:

$$\sigma(S)_{SFL} = \frac{1}{B} \cdot \sum_{j=1}^{B} \sigma_{j;SFL} \tag{5}$$

In comparison to the standard deviation of the unseparated basin σ(U) the success of the partition can be measured, e.g. as the quotient of these values.

2.3.4 An algorithm for automated sub-basin ascertainment

At this point two individual techniques, the objective function and the evaluation scheme have been established. Now these components have to be arranged in a reasonable order to perform an automated sub-basin ascertainment. Two basic considerations have already been mentioned in the introduction of the tool:

1. If low variance regions are present, these regions are clipped (by separation tool) from the rest of the basin.
2. In case of present high variance regions solely subdivision at ramification and zonal classification are carried out in competition, since the origin of high variance is unknown

Obviously, before one of these cases can be rated true the objective function has to be called. This leads to the fundamental sequence that first the objective function is called and based on the outcome, case 1 or 2, required tools are activated. Second case also requires the call of the evaluation scheme, since we have to decide which subdivision tool is more effective:

3. Results of the technique (subdivision or zonal classification) yielding a lower σ(S) will be saved, other results will be discarded.

With this consideration only some sub-basins will comprise zonal classifications, giving an inconsistent result. In order to obtain consistent results zones have to be calculated for all sub-basins:

4. Zonal classification is called additionally in case only low variance regions are present. Thereby, independent from the need of σ reduction, all ascertained sub-basins will comprise a zonal classification.

Independent from all above mentioned considerations we assume that the presence multiple major streams within a single basin requires subdivision independent from variance compulsion. Major streams can be identified and subdivided by their flow accumulation (see Appendix A for further detail). With this assumption we account for the need, e.g. to gauge or model these major streams separately. Giving the following consideration for the sequence:

5. If multiple major streams are present, the subdivision at ramification is activated without calling the objective function.

Based on the outlined considerations the sequence of the ACS (Ascertainment by Characteristic Structure) algorithm has been developed. It is depicted as a flow chart in Fig. 8.

Applied to a catchment with known coordinates of the outlet, the algorithm starts at this point. First it will check if multiple major streams are present and if necessary subdivide at ramification. Then the objective function is called and the required tool is activated. Each sub-basin will be analysed repeatedly until no SFL-class above Ω is left, or no further reduction can be generated. Please note that the described sequence is based on the presumption that shifts and breaks in the average of the characteristics along the SFL-axis are dispensable.

3 Results

Sub-basin ascertainment has been carried out on two characteristics: pore volume (total pore volume for Mulde, Regen and Main, AWC for Salzach (due to data availability, compare Fig. 2 & Fig. 3)) and surface slope. Please note that both applications and, hence, their results are disjoint.

Sub-basins and zones for all watersheds ascertained by the ACS-algorithm are depicted Fig. 9. The characteristic structure of σ(Unstructured) (blue lines) and σ(Structured) (red lines) as well as threshold Ω (according to Eq.(3)) for different weightings e = 0, e = 0.5 and e = 1 are shown in diagram. Drainage points of the defined sub-basins are classified by their derivation. Points at major ramifications are depicted as black triangles, while blue dots indicate points for separation of low variance regions and subdivisions at ramifications with order 1. These points are merged as category 1 points. Category 2 points indicate points of subdivision of higher order and hence indicate the separation of smaller contributing streams.

Although the success and differences between the outcomes of the algorithm are visible, we are still not able to quantify these observations. To make our results commensurable two numerical measures of success were developed. Both measures are based on the objective function and the evaluation scheme (Sec. 2.3.1 and 2.3.3) that imply minimisation of σ. In this cases (objective function and evaluation) only minor sets of distance classes are considered. To evaluate the performance of the algorithm within the entire catchment, all distance classes within the original, unseparated basin have to be considered.

Therefore Eq. (5) is applied to the stream-flow axis of the entire catchment and the ascertained sub-basins. The total reduction of the standard deviation σ is e expressed as the subtraction of σ(U) and σ(S). To account for different expected values of the input data (in this case a lower value for slope than for storage) the reduction of σ is normalized by the sum of initial standard deviation σ(U). The first measure is therefore the relative reduction of variance within the entire basin α_1:

$$\alpha_1 = \frac{\sum_{j=0}^{N_{sfl}} \sigma_j(U) - \sigma_j(S)}{\sum_{j=0}^{N_{sfl}} \sigma_j(U)} \tag{6}$$

With this measure we can quantify the success of a performed separation, by comparing remaining and initial heterogeneity. However, α_1 does not necessarily tell if our target has been reached. For this purpose a second measure has been established as the ratio between the remaining standard deviations σ(S) and σ(U) above the threshold Ω. For its calculation only distance-

classes comprising standard deviation greater than Ω are taken into account. The set of distance-classes fulfilling this requirement can be written as:

$$Z = [j_{sfl;1}, \ldots j_{sfl;n} \mid \sigma_j \leq \Omega] \tag{7}$$

Note that set Z is defined for the initial basin Z(U) and for the structured basin after application of ACS as Z(S). Second measure α_2 can then be written as:

$$\alpha_2 = \frac{\sum_{i \in Z(S)} \Omega - \sigma_i(S)}{\sum_{j \in Z(U)} \Omega - \sigma_j(U)} \tag{8}$$

Values of proposed measures can be interpreted as follows: The higher the total reduction α_1 and the lower the remaining variance above the threshold α_2, the more heterogeneity could be compensated by the algorithm.

Keep in mind that these success rates examine the performance of the algorithm for a completed ascertainment. This is contrary to the evaluation of tools (Sect. 2.3.3) which only considers a single subdivision/separation.

Calculated α_1 and α_2 values for all applications are tabulated in Table 1. These values and the depiction of the results in Figure 9 shows that some applications were more successful than others, e.g. application on pore volume data in the Main catchment (nearly all classes below Ω, best α_1 and α_2) compared to slope for the Mulde basin (lowest α_1 and only few classes under Ω). The density of close to stream zones is comparable for all basins, it ranges from 18 – 25 % for pore volume and 22 – 30 % for slope.

However, application on pore volume in all basins led to significantly higher success rates than for slope values. Another striking result is the outcome in the Salzach catchment. While the application of pore volume resulted had the lowest success, the application on slope has been more successful, especially α_2 is with 67,2% significantly higher than for all other slope applications. The opposite is visible in the results of the Mulde, while application of pore volume led to average reduction for both parameters, slope application led to the lowest (total) reduction values. Generally it is visible (Fig. 9 and Tab. 1) that the standard deviation σ(S) could be reduced in all basins and for both data applications.

4 Discussion

4.1 Limiting factors for the algorithm

In this section we will examine the results of spatial subdivisions obtained with the ACS algorithm. A special focus is set on catchment properties that affected the performance and hence define the outcome of the algorithm. Therefore we have to identify in which basins the algorithm performed well and in which it did not.

It is striking that applications on pore volume led to significantly higher reductions than applications on slope data. While the total reduction for pore volume ranges from 41 to 65 %, variance of slope could only be reduced in a range from 10 to 28 %. Though α_2 ranges intersect, the average α_2 for pore volume is superior to slope application. Nevertheless, low success rates

seem not to be limited to one catchment, but rather to the observed feature. These observations give first hinds to the question which catchment property, or properties, affect the performance of the algorithm and hence define its results. Possible explanatory factors are the geomorphologic structure and/or the specific values of the considered features.

With our case study catchments we cannot prove these assumptions distinctly since structure and range of values are different. Especially the geomorphologic structures are nearly incomparable. To handle this problem we performed a resampling experiment. The basic concept is to examine structural identical catchments with a different range of featured values. First step is to examine the spatial organisation of pore volume in the Mulde as it is. Then we change the specific values of pore volume and repeat the analysis. If performance measures α_1 and α_2 are similar, the assumption about dependency of performance on the range of values has to be rejected.

In order to change featured values in a reasonable way, we did not change the values randomly but exchanged data of two natural catchments. Accounted by their similar size, the Mulde and the Salzach catchment were chosen for resampling. The exchange of pore volume between these two catchments has to retain the order and arrangement of the original catchments. Therefore we assigned high pore volume values of the original basins to high pore volume values in the exchange basin and applied this scheme to all values. Then the values were exchanged. The same exchange of values has been applied to the DEM, as the root of slope values. Figurate, the alpine structure of the Salzach has been shifted to soil and heights of the Ore Mountains, and the middle mountainous structure of the Mulde to an alpine soil and topography. If the performance in these resampled basins is identical to the performance in their origin basin (e.g. resampled AWC Mulde and original AWC Salzach) the assumption about dependency of performance on geomorphologic structure has to be rejected.

Resampled AWC values are shown in Fig.10. Stream network, SFL- and slope values were recalculated for the new DEM. Afterwards the ACS algorithm has been applied to the resampled basins. Results are shown in Fig. 11 and the success rates are given in Table 2.

If the characteristic structure for pore volume in the unseparated original catchments $\sigma(U)$ (Fig. 5 (Mulde) and Fig. 9 (Salzach) are compared to the resampled structure of $\sigma(S)$ (Fig. 11) a difference is visible. On the one hand the absolute values of standard deviation has changed and on the other hand the succession and arrangement of these values has changed. In case of slope data only the absolute amount of standard deviation has changed while the succession of values is nearly identical. A comparison of α_1 and α_2 values (Tab. 1 and Tab. 2) in the original and resampled basins shows that performance in the Mulde catchment slightly decreases or is stable, while it increased in the Salzach basin (with exception to α_1 for pore volume which decreases by 8%).

As it can be seen in the characteristic structures, the range of σ of the Mulde catchment is similar to the range of σ in resampled Salzch basin and vice versa. Hence, the alteration of absolute standard deviations is directly caused by the performed exchange of values. Characteristic structures $\sigma(S)$ of resampled and original pore volume in the Salzach basin differ in the missing peaks of $\sigma(S)$. Generally resampled $\sigma(S)$ is more equally distributed than in the original basin. Contrary to this, $\sigma(S)$ in the resampled Mulde basin has a distinct peak of standard deviation at about 80-100 km distance from the outlet. These modification can be explained by the soil arrangement of the Salzach catchment.

Figure 12 shows a map of (original) AWC in the Salzach catchment in a larger scale. In this figure three regions within the catchment are marked with red squares. These regions comprise soil heterogeneities that can be described as small enclosures of high pore volume values. These enclosures differ significantly from their surrounding soil and do not follow the co-evolutional structure of the remaining basin. Since these enclosures cause variations they are visible in the characteristic structure of the basin (right hand side of Fig. 12). With the transition of more uniform pore volume values from the Mulde basin, these enclosures vanish and hence the peaks in the structure. Consequently the high values of the enclosures are transferred to the Mulde, these spots are best visible in Fig. 10, located in the upper region on the right boundary of catchment. The placement of high value enclosures in the resampled Mulde catchment is the explanation for the reduction of performance α_2. In the Salzach catchment, the total variance reduction decreased. Because the value of $\sigma(U)$ resampled and original are similar, the lowered variance $\sigma(S)$ in the resampled basin causes this decrease. Nevertheless, the remaining variance above the threshold α_2 is lowered by 13.1%. In the resampled Mulde basin α_1 is nearly stable which is due to the fact that the enclosures are merged into a single, wider spot.

Following this discussion a first limitation can be stated: enclosure of values that do not follow the flow path arrangement of the catchment lower the ascertainment success rate. Moreover the difference between the actual values in the enclosure and the surrounding values has an impact on the performance. The higher the difference the lower the success rate.

In case of the resampled slope values the success rates have changed only slightly (maximum alteration 8%) and the shape of characteristic structures for separated $\sigma(S)$ and unseparated basins $\sigma(U)$ are nearly identical in the original and resampled basin. Only the actual range of standard deviation has changed. This outcome indicates that the actual range of standard deviation does not affect the performance of the algorithm. Moreover, in accordance to the beforehand drawn conclusion the geomorphologic structure can be identified as the main influencing variable defining outcome and performance of the algorithm. Hypothesis about dependencies between results and the range of featured values has to be rejected.

However, results also show that the performance for application on slope data is always inferior to applications on pore volume. The only reasonable explanation is that catchment characteristics directly bound to the structure (differences in heights define the flow path) cannot be encompassed properly by the algorithm in its present state.

In summary the application of the ACS algorithm to four different natural catchments and the resampled basins succeeded. Hypothesis about the influence of geomorphologic structure could not be rejected. Contrary to that we could show independence of the outcome from the range of catchment characteristic values. Nevertheless results indicate that the algorithm is not limited to a single catchment structure or range of values. As a major factor affecting the performance of the proposed algorithm the occurrence of soil enclosures, or in general term the occurrence of spots that differ significantly from the surrounding values has been identified. Their affection on performance is dependent on the actual deviation between the enclosure and its surroundings.

4.2 Spatial extend of zones

Although the subdivision and separation tools are, in the sense of σ-reduction, mostly superior to zonal classification (what can be concluded from the high number of performed sub-divisions and, in relation to the initial basins, small sub-basins) a look at the spatial extend of zones is worthwhile. For this analysis we are looking at the "close to stream" zones, since "far from stream" zones are calculated as remaining cells. Results (Table 1 and Fig. 9) show that the average extent of "close to stream" zones is similar in all catchments and for both applications. Nevertheless, differences are visible between the sub-basins within these watersheds. Neighbouring and nested sub-basins reveal in some cases significant differences although their spatial allocation might suggest different. While some sub-basins are separated in small close to stream belts around the major streams and large "far from stream" zones, others incorporate extensive "close to stream" zones. The zone densities, calculated as the proportion of "close to stream" zones of the entire (sub-)basin, within all applications have an average of 24% but the range of densities moves from 0.5% to 67%. This observations leads to a fundamental question: Which properties of the basins surface, i.e. physiographic property regulates extend of these zones?

To answer this question we have to look into more detail of the results. Since the target of zonal classification is to reduce σ of the sub-basin by separating into two sets of values, there are two ways to cope with this task. Either the "close to stream" zone tries to cover as much cells as possible with a minimum of variance, or it tries to embrace regions of the sub-basin casing a maximum of variance with a minimum of coverage. These two operations of zonal classification can be called "Minimisation" and "Maximisation". In Fig. 13 the usage of these operations is shown on the example of the Mulde. Extend of zones is perceivable not bound to the operation. If we now take the relationship between standard deviations in "close to – " and "far from stream" into account, see right of Fig. 13, a pattern becomes visible. While narrow zone belts around streams tend to comprise a high quotient of standard deviations, extensive zone are mostly present if the quotient is low. Results of the other basins are not shown here, but imply identical interpretations.

These findings can answer the initial question: Extend of zones is bound to the presence of patterns around the major streams within a catchment. In the absence of a clear stream orientated pattern, "close to stream" zone get more extensive.

4.3 Comparison to gauging networks

After the evaluation of functionality the usefulness of the proposed algorithm has to be evaluated. One possible field of application is the use for semi-distributed hydrological models or as reference subdivision for the examination of existing gauging networks. In both applications defined sub-basins, defined by modelling nodes or gauges, are defined to reduce the catchments heterogeneity and to model or observe discharge from mostly homogenous regions. Obviously, existing gauging networks are a result of multiple considerations and requirements and in some parts of the basin tend to be denser than required to catch the natural heterogeneity of a single catchment characteristic. On contrary, due to its multiple requirements, the gauging network is not orientated on a single characteristic and will always represent a compromise of possible decisions. A comparison to results of the ACS algorithm is therefore not in all cases fair. Nevertheless, differences in the number of

separation points, or the reduction of variance can give hinds to decision makers for possible new gauging positions. The usefulness for the decision maker is bound the informational value of the specific catchment characteristic for runoff generation processes.

However, for our purpose, the evaluation of the ACS algorithm we assume that pore volume and slope are crucial information. To evaluate the power of the ACS algorithm two comparisons are performed. First, a subdivision based on the gauging network will be compared to the obtained basins (without ACS zones) introduced in Sec. 3. With this analysis it will be possible to evaluate the power of defined separation points. A Second comparison will use the basins and zones introduced in Sec. 3 compared to a subdivision based on the gauging network and a zonal partition by land cover. Based on the suggestions by Lindström et al. (1997) land cover has been merged into two categories: field and forest. Additionally a third zone Rock / Bare soil has been introduced, which has been considered necessary for the Salzach catchment. Although the simple land cover omits the exact allocation of the zones, due to its simplicity and common usage it appeared to be adequate. By introduction of this classification a fair benchmark has been set up for comparison. The gauging network and defined land cover zones are shown on the left of Fig. 14

The measure of success (Eq. 5) has been applied to these subdivisions and the characteristic structure of $\sigma(S)$ for pore volume and slope were determined. Characteristic structures for gauging network (blue) and land cover (green) partition are depicted in the middle and on the right of Fig. 14. For visual comparison the characteristic structure of ACS basins (red) are added in the figure. Success rates $\alpha 1$ (Eq. 6) and $\alpha 2$ (Eq. 8) were calculated and presented in Tab. 3.

If we compare results for ACS-basins only and the gauging network in Tab. 3 it is visible that the success rates are significantly higher for ACS basins. In average the reduction of the standard deviation α_1 for both variables is 50% higher and the remaining standard deviation above the threshold α_2 is 32% lower. This difference has two reasons: On the one hand for some basins more separation points than gauging points have been defined. On the other hand the adjustment of separation points on the specific variable itself led to less points than the gauging network. The first case is a hind for a necessary extension of the gauging network (or node-network) and the second case either approves the existing network or indicates better positions for existing gauges / nodes.

For a second analysis the analysed sub-basins are subdivided into zones by ACS classification and land cover zones. Performance of sub-basins ascertained by gauging network and land cover zones is treated as benchmark for the ACS algorithm. In Fig. 14 it is visible that ACS (red) results give lower or equivalent $\sigma(S)$ values to the benchmark partition (green) for pore volume application. This observation is confirmed by success rates given in Tab. 1 and 3. Average advantage of the ACS is 42% for α_1 and 66% for α_2. Contrary to this result, application on slope shows that the benchmark is, with exception of the Regen catchment, superior to the ACS results (15% for α_1 and 30% for a_2).

Since the comparison of sub-basins solely showed that ACS is superior to the benchmark, the explanation for this result is the usage of land-cover zones. These zones are independent from the structure of the basins and could possibly give a better, or at least an alternative way to assess network bound parameters. This results indicates a need for further improvement of ACS-classification. For example a third category based on land use or heights might be beneficial.

Ascertained sub-basins have been compared with the elaborate technique of stream flow orientated standard deviation, introduced by ourselves. Obviously this is not an acceptable validation of the proposed method. Since a fully-fledged validation is dependent on the purpose, e.g. performance in a hydrological model, regionalisation scheme etc. (which would go beyond the scope of this paper) we have to address the validation on a basic level. But how are different spatial resolutions commonly compared? A possible and plain answer is to compare the average of variation (for considered characteristics) within the sub-basins.

For this analysis we took the sub-basins ascertained by ACS and the gauging network and omitted the zones. For each sub-basin the plain standard deviation of pore volume and slope has been calculated. Table 4 shows the area weighted averages of these values per catchment and the relative advantage of ACS sub-basins. The advantage ranges from 1.4 to 15.1% which is a rather low advantage. Yet it has to be taken into account that zones have been neglected and the attention of this study is set on the flow path.

4.4 Definition of physiographical types

As mentioned in the introduction the proposed algorithm accounts for the spatial organisation of the catchment and the interaction with the catchment characteristics. Hence, its results should incorporate information about the spatial organisation and information about the lateral flow path. Grayson and Blöschl (2001) pointed out that these information could give insight to processes of lateral flow distribution. Therefore it seems worthwhile to establish a similarity measure for sub-basins ascertained with the ACS-algorithm. In this section we will give a prospect on a possible classification scheme which could be used for regionalisation studies.

The test of general applicability (Sec. 3) yielded sub-basins and zones for different catchment characteristics. To assess the similarity of these results (to assess the spatial organisation) these results have to be combined. The simplest way to combine the outcome of different input data, and retain the univariate objective function, is to run the algorithm in turn over all input data and use ascertained sub-basins as pre-subdivision. Afterwards a combined set of sub-basins is obtained that accounts for all input data. In order to obtain zones for these sub-basins, the algorithm has to be rerun for all input data, using the beforehand obtained sub-basins. Individual zone networks are available for each catchment feature after this procedure.

To combine them it seems worthwhile to overlay the obtained data sets. Figure 15 shows the overlay of zones for slope (yellow) and pore volume (blue) for all catchments used in this study. Intersecting zones appear greenish. It is now up to the user to decide how these zones are combined. Either they can be combined through logical operators (intersection or union) or as weighted averages by means of weights of the input data or by the reduction of variance of each zone.

Beside the combination of zones they could be used for the assessment of spatial organisation of catchments. After the application of the algorithm we assume that each sub-basin certainly represents a homogeneous natural unit. Defined zones indicate the structure of the input data with respect to drainage system within this unit (compare Sec. 4.2). Following the definition of Winter (2001) a hydrological landscape is determined by the interaction of a physiographic feature and the

hydrologic system. The physiographic part is defined by its land surface form, the geological system and its climate. The hydrologic system defined by surface, ground and atmospheric water.

With the conducted case studies, we are able to use the slope data as information about the flow energy and the pore volumes as information about the pedologic system and, hence, are able to identify similar patterns of surface morphology. Similar patterns are classified into physiographical types.

If Fig. 15 (left side) is examined with this perspective four types of zonal intersections are visible:

- Type A: Narrow slope and pore belts. Soil is arranged in valleys along main rivers. Especially visible in map excerpt I in Fig. 15 (right side).
- Type B: Soil belts and extensive slope zones. Soil patterns are bound the drainage system, with disseminated side-arm valleys, or plains.
- Type C: Slope belts and extensive soil zones. Valleys around the main rivers with similar to hillslope soils.
- Type D: Plains or disseminated side-arm valleys with no predominant soil pattern. Shown in map excerpt II in Fig. 15 (right side).

In map excerpt A in Fig. 15 we can see a wide valley, with sloping hillsides, the AWC follows this patterns with higher values in the stream valley. “Close to stream” zone densities (left side of Fig. 15) are low and shaped like a single line. In contrast, map excerpt B shows a shallower, disseminated valley with no soil pattern. These two excerpts are good examples for Type A and D sub-basins.

To derive a physiographic type for a certain sub-basin its zone densities have to be rated has high or low. Therefore a k-Means analysis has been carried out for an, as much as possible, impartial differentiation between high and low densities. Boundary values were found in a range from 22% to 27% zone density. A scatterplot of zone densities in the Salzach catchment and the calculated k-means boundaries are shown in Fig. 16. The four sectors can be interpreted as the four defined physiographical types: Type A in the lower left, Type B upper left, Type C lower right and Type D in the upper right.

This classification schemes has been applied to all catchments. The obtained maps of present physiographical types are shown in Figure 17. In the Mulde catchment types A and B are predominant while in the Regen catchment type B is dominant solely. While the Main catchment is dominated by C and D types, the Salzach catchment is split into a Type A dominated part and mixed section.

In summary the automatically ascertained sub-basins and zones have been used to categorize regions of catchments into different physiographical types. These types were designed to represent different surface and soil patterns. For the actual categorisation we used the density of defined zones and used gathered information (Sec. 4.2) about the link of stream network patterns and zone density to derive a classification scheme. However, the absence of an impartial threshold required the (more or less) subjective choice a threshold value for classification of the sub-basins. Therefore the presented results have to be considered as a prospect to future work and possible applications of the algorithm.

5 Conclusions

A new approach for the analysis of watersheds based on the interaction of catchment characteristics and the flow path has been introduced in this study. Based on this method an algorithm has been proposed for automated and impartial sub-basin ascertainment. This new methods and algorithm detect and incorporate the spatial organisation of the watershed into the definition of sub-basins and zones. General Applicability on different catchment characteristics and different catchment structures has been shown in a case study. The proposed ACS algorithm has been applied to topography and soil data of four meso-scale watersheds. Results showed that the performed subdivisions delivered a reasonable number of sub-basins and could significantly reduce the heterogeneity of the considered characteristic within these sub-basins. A detailed analysis, incorporating a numerical resampling experiment, could additionally detect some limitations for the ACS-algorithm. Especially the occurrence of soil enclosures, incorporating properties that differ significantly from their surrounding soil, could be identified as interfering. But the occurrence of these enclosures does not always led to significant reduction of the success rate, but rather the heights of the difference between the enclosure and its surrounding were identified to be important. Performed applications and experiments could show that geomorphology has an impact on the performance of the algorithm. But its general applicability is not limited to a single catchment structure. Additionally we could show that characteristics directly bound to the catchment structure (i.e. flow path) could not be encompassed sufficiently. Although limitations have been identified, the proposed techniques performed well in our case studies.

Its performance, in sense of flow-path orientated standard deviation has been compared to the common strategy of sub-basin definition based on the gauging network and land cover classification. It could be shown that sub-basins ascertained by the proposed algorithm inhibit a significantly lower variation along the flow path. Furthermore a prospect on the usage of the algorithm and its outcomes for modelling and regionalisation purposes has been given. In comparison to the employed benchmark methods (and other methods) some advancements of the proposed method and algorithm can be pointed out. First, the underlying method of characteristic structures which accounts for the occurrence of catchment characteristics by their distance to the outlet differentiated between stream flow length and over land flow length. This approach employs more information about a basin than other common pattern identification schemes, like point-to-point comparisons or optimal logical alignment (Grayson and Blöschl, 2001). Nevertheless, the full benefits of these advancements for different hydrological purposes is still outstanding and will be addressed in upcoming research.

Second, the ACS-algorithm incorporates three techniques for sub-basin ascertainment and accounts for the interaction and succession of different catchment characteristics. This is a major advancement to common subdivision methods which are based only on the stream network, via Pfafstetter codification (Verdin and Verdin, 1999) or by Strahler order (Rodríguez-Iturbe and Valdés, 1979). Other methods that do account for surface characteristics are usually HRU concepts (Winter, 2001; Wagener et al., 2007; Schumann et al., 2000; Winter, 2001) that neglect the allocation of coherently alike regions and their succession within the catchment. Although ACS incorporates a zonal classification that is comparable to an HRU concept, the

defined zones do retain the order within the sub-basin in sense of the flow path. The concept is most likely comparable to the concept of Nobre et al. (2011).

More specifically, the ACS-algorithm defines two zone types within each sub-basin to account for stream network orientated patterns. Since we assumed that the algorithm produces homogeneous natural units the density of zones has been used to define independent physiographical types as part of hydrological landscapes (Winter, 2001). As a measure of physiographical similarity we used the spatial extend of "close to stream" zones, since they indicated the presence of stream network orientated patterns. In this paper only two variables were used and hence only two zone types and four physiographical types were identified. A additional variables are the height above the nearest drainage (Nobre et al., 2011) in order to account for plateaus within the catchment and the hydraulic conductivity of soils.

However, the obtained results only give physiographical similarity of the sub-basins. Future work has to account for the hydrologic system and has to compare the hydrologic similarity to the physiographic similarity. With this intersection the utility of the proposed method for the description hydrological landscapes could be evaluated and elaborated to a catchment classification scheme. In contrast to other schemes (e. g. 2010; Sawicz et al. 2011 and Winter, 2001) the derived landscape types are not derived by statistics about the sub-basin but by its spatial organisation.

Appendix A

In this Appendix details to the proposed ACS-tools are given for further understanding of the algorithm. Each tool will be addressed separately.

Separation tool for low variance regions

Low variance regions have no need for further subdivisions. Therefore they are separated from the rest of the basin. Since the exact allocation of these regions is known, all cells within can be defined as target area T (hatched in Fig. 7, upper left side). Remaining cells are drawn together as non-target area NT. If one random point of the basin is selected as possible separation point (SP) and its watershed is calculated the set of points belonging to the watershed, or sub-basin, of SP, BSP is obtained. The calculated watershed BSP covers parts of T and NT and hence a coverage rate can be calculated as the proportion of the cardinalities of the intersections and their respective superset:

$$C_{SP} = \frac{\left|B_{SP} \cap T\right|}{\left|T\right|} - \frac{\left|B_{SP} \cap NT\right|}{\left|NT\right|} \rightarrow \max \qquad \text{(A1)}$$

The objective of a separation C is to find a separation point (SP) whose basin BSP covers a maximum of T and a minimum of NT. Please note that for regions located at the outlet of the basin or at its upstream boundary only one SP will be defined. Possible SPs are assumed to be allocated at the transit of the main stream from T to NT, or vice versa. An iterative search

returns the coverage values C and the highest value is selected as SP, defining a new sub-basin. In the upper part of Fig. 7 a concluded separation, as well as the rejected SPs of the iteration (hollow points) are shown.

Subdivision at confluences/ramifications

Because the chosen perspective is upstream, the ACS is searching for ramifications of the river network, where a main river splits into two tributaries. To identify ramifications the characteristic structure of flow accumulation (FAcc) is examined. Since the FAcc indicates the contributing drainage area to each stream cell, discontinuities in the characteristic structure, which is the succession of the FAcc values, will reveal confluences of streams.

Figure A2 shows an example for the Mulde. Beginning at the Outlet (zero on the x-axis) two features are visible: a slowly decreasing line of high FAcc values, representing the main stream at the outlet, and a noise-like smaller range of FAcc values close to the abscise, caused by the smaller tributary streams and contributing areas. To identify major tributaries this noise has to be removed. We assume that in the first distance class the disparity between main rivers and contributing hillslopes is most distinct. Within the first SFL-class a k-Means cluster analysis is carried out to divide high and low FAcc values. Threshold value τ_S is determined as:

$$\tau_S = \min_{c}\left[\max_{c1}\left[FAcc\right];\max_{c2}\left[FAcc\right]\right]\cdot\left(1-\frac{i}{10}\right) \quad \text{(A3)}$$

where c indicates the clusters and i is the reduction order and by default 0. The algorithm will start with the default value for i and searches for the first ramification in upstream direction. If no ramification is found, order i is increased by 1. The maximum order is set to 10. Please note that the higher i is set, the lower the threshold gets and more FAcc-values remain for analysis. The routine identifies the coordinates of the ramification inducing the drop in FAcc values (see Fig. A2, for example at SFL ≈ 80 km).

Drainage points of Major streams, or major stream ramifications are identified likewise. Before the objective function is called, prevailing FAcc values in the basin are checked. If the FAcc value of the tributary stream is higher than the threshold value τ_R, a subdivision is performed. This parameter is calculated as percentage of the maximum FAcc value in the entire watershed (e.g. 5%) once at the initialisation of the algorithm.

Zonal classification

Another way to subdivide a high variance region without setting new separation points is to split the cells within the region, i.e. the catchment into zones. This is comparable to the concept of HRUs. But, in this case we take the allocation of each cell and its position along the SFL-axis into account. Therefore, only two possible types were implemented: “close to stream” and “far from stream” cells. For some catchment characteristics these zone might comply with natural wetlands and hillslopes, but is not compulsory for all possible input data.

To identify close to stream cells, firstly the stream has to be selected. Since, we try to emulate natural patterns of the input data not all present stream cells might be relevant. We assume that we need to separate data fields around higher order streams from

data fields located at lower order streams. Therefore, streams are selected by their Strahler order. Cells draining into the selected stream cells, with an OFL value equal or below a threshold Δo, are defined as "close to stream" cells. Remaining cells are marked as "far from stream".

Because we do not know the dominant spatial pattern of the input data the search for an optimal extent of the "close to stream" zone is done iteratively. The iteration employs two variables: the reduction of the Strahler order s_R from the maximum occurring Strahler order M_S and the width of the zones Δo, expressed as multiple of cell width. Parameter ranges are [0; M_S-1] for s_R and [0, 5] for Δo, respectively. Cells draining into streams cells with Strahler order equal or lower than M_S-s_R and an OFL value equal or lower than Δo·Δx are marked as "close to stream". In Fig. A3 a sequence of the iteration is shown for the entire synthetic catchment. After each iteration, the standard deviation σ (Eq. (2) & (5)) is calculated for each zone and subsequently averaged. The parameter combination (s_R, Δo) with the lowest averaged standard deviation is chosen for final classification. In Figure 7, an example for a chosen zonal classification for the synthetic catchment is shown. The ACS will define results of the technique leading to the highest reduction of the standard deviation σ as superior and omits the inferior result.

Please note that the algorithm has the possibility to neglect the usage of zonal classification. If the calculated averaged σ of the zones is equal to or higher than σ of the unseparated data, the whole basin will be marked as zone type "none".

References

Beven, K.: A manifesto for the equifinality thesis, Journal of Hydrology, 320, 18–36, doi:10.1016/j.jhydrol.2005.07.007, 2006.

Blöschl, G., Sivapalan, M., Wagener, T., Viglione, A., and Savenije, H.: Runoff Prediction in Ungauged Basins: Synthesis across Processes, Places and Scales, Cambridge University Press, Cambridge, 492 pp., 2013.

Bossard, M., Feranec, J., and Otahel, J.: CORINE land cover technical guide: Addendum 2000, EEA, Copenhagen, 2000.

Bremicker, M.: Das Wasserhaushaltsmodell LARSIM: Modellgrundlagen und Anwendungsbeispiele, Hochwasserzentralen LUBW, BLfU, LfU RP, HLNUG, BAFU, 2016.

Dunn, S. M. and Lilly, A.: Investigating the relationship between a soils classification and the spatial parameters of a conceptual catchment-scale hydrological model, Journal of Hydrology, 252, 157–173, doi:10.1016/S0022-1694(01)00462-0, 2001.

Gharari, S., Hrachowitz, M., Fenicia, F., and Savenije, H. H. G.: Hydrological landscape classification: investigating the performance of HAND based landscape classifications in a central European meso-scale catchment, Hydrol. Earth Syst. Sci., 15, 3275–3291, doi:10.5194/hess-15-3275-2011, 2011.

Grayson, R. and Blöschl, G. (Eds.): Spatial patterns in catchment hydrology: Observations and modelling, Cambridge Univ. Press, Cambridge, 404 pp., 2001.

Güntner, A., Seibert, J., and Uhlenbrook, S.: Modeling spatial patterns of saturated areas: An evaluation of different terrain indices, Water Resour. Res., 40, n/a-n/a, doi:10.1029/2003WR002864, 2004.

He, Y., Bárdossy, A., and Zehe, E.: A catchment classification scheme using local variance reduction method, Journal of Hydrology, 411, 140–154, doi:10.1016/j.jhydrol.2011.09.042, 2011.

Jenson, S. and Domingue, J.: Extracting topographic structure from digital elevation data for geographic information-system analysis, Photometric Engineering and Remote Sensing, 54, 1593–1600, 1988.

Lindström, G., Johansson, B., Persson, M., Gardelin, M., and Bergström, S.: Development and test of the distributed HBV-96 hydrological model, Journal of Hydrology, 201, 272–288, doi:10.1016/S0022-1694(97)00041-3, 1997.

Merz, R. and Blöschl, G.: A process typology of regional floods, Water Resour. Res., 39, doi:10.1029/2002WR001952, 2003.

Müller, C., Hellebrand, H., Seeger, M., and Schobel, S.: Identification and regionalization of dominant runoff processes – a GIS-based and a statistical approach, Hydrol. Earth Syst. Sci., 13, 779–792, doi:10.5194/hess-13-779-2009, 2009.

Nobre, A., Cuartas, L., Hodnett, M., Rennó, C., Rodrigues, G., Silveira, A., Waterloo, M., and Saleska, S.: Height Above the Nearest Drainage – a hydrologically relevant new terrain model, Journal of Hydrology, 404, 13–29, doi:10.1016/j.jhydrol.2011.03.051, 2011.

Rodríguez-Iturbe, I. and Valdés, J. B.: The geomorphologic structure of hydrologic response, Water Resour. Res., 15, 1409–1420, doi:10.1029/WR015i006p01409, 1979.

Savenije, H. H. G.: HESS Opinions "Topography driven conceptual modelling (FLEX-Topo)", Hydrol. Earth Syst. Sci., 14, 2681–2692, doi:10.5194/hess-14-2681-2010, 2010.

Sawicz, K., Wagener, T., Sivapalan, M., Troch, P. A., and Carrillo, G.: Catchment classification: empirical analysis of hydrologic similarity based on catchment function in the eastern USA, Hydrol. Earth Syst. Sci., 15, 2895–2911, doi:10.5194/hess-15-2895-2011, 2011.

Schumann, A., Funke, R., and Schulz, G.: Application of a geographic information system for conceptual rainfall-runoff-modeling, Journal of Hydrology, 45–61, 2000.

Sivapalan, M.: Pattern, Process and Function: Elements of a Unified Theory of Hydrology at the Catchment Scale, in: Encyclopedia of hydrological sciences, Anderson, M. G. (Ed.), Wiley, Chichester, 193–219, 2005.

Sivapalan, M., Takeuchi, K., Franks, S. W., Gupta, V. K., Karambiri, H., Lakshmi, V., Liang, X., McDonnell, J. J., Mendiondo, E. M., O'Connell, P. E., Oki, T., Pomeroy, J. W., Schertzer, D., Uhlenbrook, S., and Zehe, E.: IAHS Decade on Predictions in Ungauged Basins (PUB), 2003–2012: Shaping an exciting future for the hydrological sciences, Hydrological Sciences Journal, 48, 857–880, doi:10.1623/hysj.48.6.857.51421, 2003.

Skøien, J. O., Merz, R., and Blöschl, G.: Top-kriging - geostatistics on stream networks, Hydrol. Earth Syst. Sci., 10, 277–287, doi:10.5194/hess-10-277-2006, 2006.

Soulsby, C., Tetzlaff, D., Rodgers, P., Dunn, S., and Waldron, S.: Runoff processes, stream water residence times and controlling landscape characteristics in a mesoscale catchment: An initial evaluation, Journal of Hydrology, 325, 197–221, doi:10.1016/j.jhydrol.2005.10.024, 2006.

Sponagel, H. (Ed.): Bodenkundliche Kartieranleitung: Mit 103 Tabellen und 31 Listen, 5., verb. und erw. Aufl, Schweizerbart, Stuttgart, 438 pp., 2005.

Verdin, K. and Verdin, J.: A topological system for delineation and codification of the Earth's river basins, Journal of Hydrology, 218, 1–12, doi:10.1016/S0022-1694(99)00011-6, 1999.

Wagener, T., Sivapalan, M., Troch, P., and Woods, R.: Catchment Classification and Hydrologic Similarity, Geography Compass, 1, 901–931, doi:10.1111/J.1749-8198.2007.00039.X, 2007.

Winter, T. C.: The concept of hydrological landscapes, J Am Water Resources Assoc, 37, 335–349, doi:10.1111/j.1752-1688.2001.tb00973.x, 2001.

Table 1: Results of applications of *ACS*. Number of ascertained sub-basins, normalized reduction of standard deviation σ and density of close to stream zones.

	Pore Volume				**Slope**			
Catchment	No. of Basins[-]	α_1 (Eq. 7) [%]	α_2 (Eq. 9) [%]	Close to stream zones [%]	No. of Basins [-]	α_1 (Eq. 7) [%]	α_2 (Eq. 9) [%]	Close to stream zones [%]
Mulde	70	52.2	69.8	22.3	80	10.6	49.0	22,1
Main	59	64.5	82.9	25.8	22	19.3	26.9	26.5
Regen	17	52.8	70.2	18.8	24	16.1	28.9	30.1
Salzach	24	41.0	56.8	20.9	38	18.4	67.2	24.4

Table 2: Normalized reduction of standard deviation σ for resampled basins

Catchment	Pore Volume		Slope	
	α_1 [%]	α_2 [%]	α_1 [%]	α_2 [%]
Mulde (res)	54.7	69.2	8.5	51.1
Salzach (res)	33.4	32.8	20.9	68.0

Table 3: Normalized reduction of standard deviation σ for sub-basins based on gauging network, ACS-basins and gauges and land cover

Catchment	Pore volume		Slope		No. of Gauges
	α_1 [%]	α_2 [%]	α_1 [%]	α_2 [%]	
Gauging network					
Mulde	24.2	57.7	9.4	43.3	40
Main	41.9	81.1	14.0	15.8	46
Regen	18.9	54.9	6.5	17.4	20
Salzach	30.3	49.6	9.6	58.6	33
ACS-basins only					
Mulde	39.2	59.4	13.7	44.9	70/80
Main	55.8	79.8	14.7	19.8	59/22
Regen	41.3	61.4	11.5	27.2	17/24
Salzach	31.3	48.1	11.9	61.3	24/38
Gauging network & land cover					**Occ. zones**
Mulde	35.3	62.8	14.5	43.1	2
Main	48.9	84.6	19.8	18.8	2
Regen	25.1	58.5	14.3	19.5	2
Salzach	38.4	64.6	21.6	66.8	3

Table 4: Averages of plain standard deviation for sub-basins ascertained by ACS and gauges

	Pore Volume [mm]			Slope [°]		
Catchment	ACS	Gauges	Diff.	ACS	Gauges	Diff.
Mulde	131.7	142.7	7.7%	2.7	3.2	15.1%
Main	155.5	158.8	2.1%	3.9	4.1	1.4%
Regen	90.5	105.7	14.4%	4.2	4.1	3.0%
Salzach	155.5	158.9	2.1%	3.9	4.1	1.4%

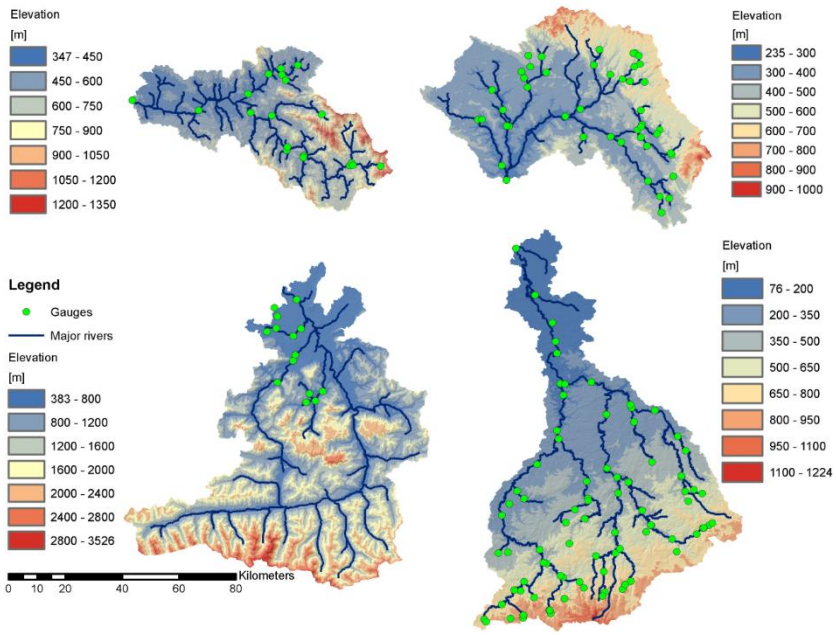

Figure 1: Digital Elevation models of the Regen (upper left) and upper Main (upper right) both in Bavaria, Germany, Salzach (lower left) in Salzburg, Austria, and the Mulde (lower right) in Saxony, Germany.

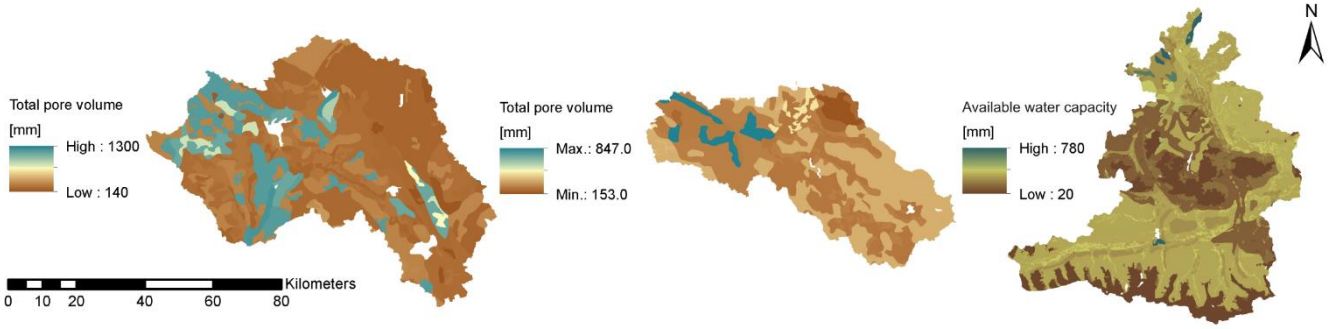

Figure 2: Values of total pore volume in the catchment of Main (left), Regen (centre) and available water capacity for catchment of Salzach (right)

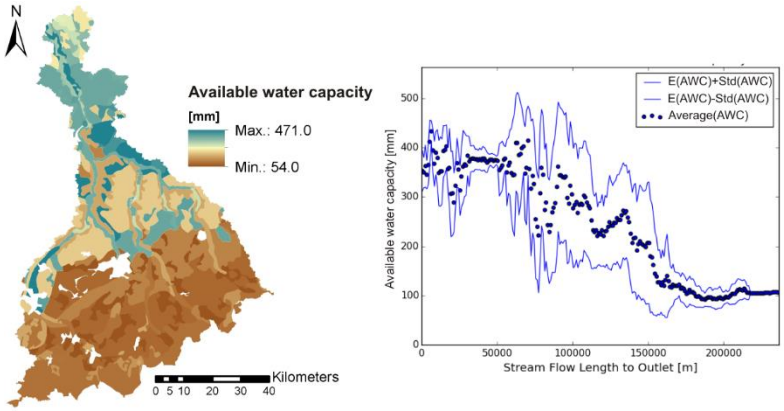

Figure 3: Available water capacity in the Mulde catchment (left) and calculated characteristic structure (right)

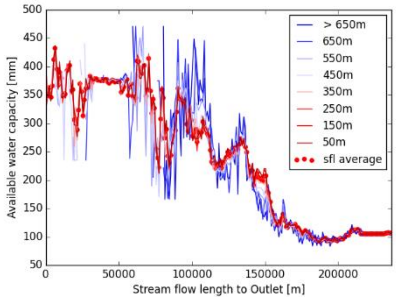

Figure 4: Average AWC in OFL classes in the Mulde catchment

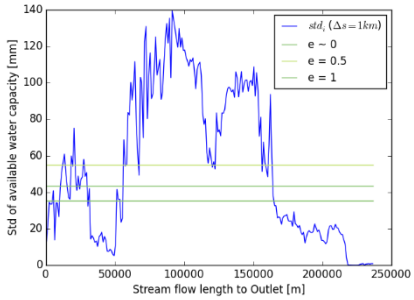

Figure 5: Standard deviation σ(AWC) in SFL-classes and Threshold values τ_S for different values of *e*, in the Mulde catchment

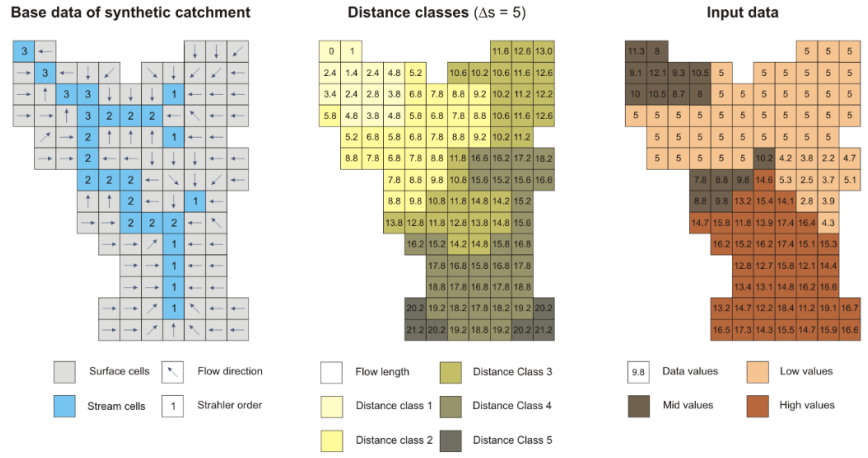

Figure 6: Flow direction and Strahler order (left), SFL-data and –classes (middle) and example input data (right)

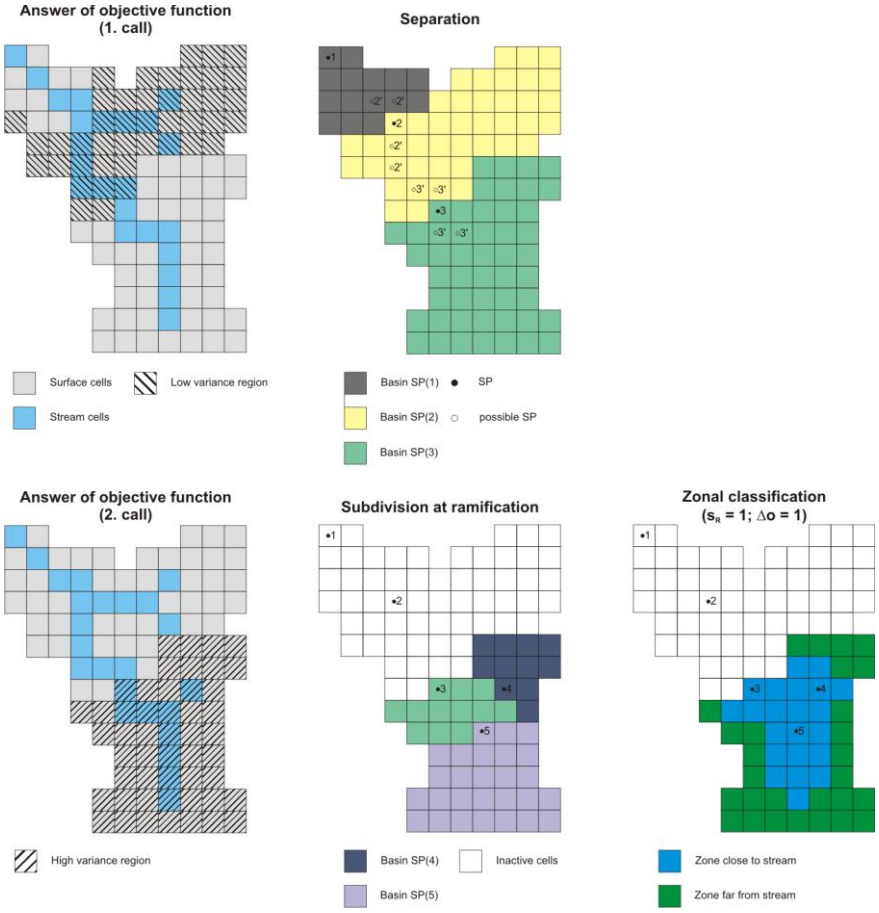

Figure 7: Answers of the objective function (left) and separation (upper right) and subdivision techniques (lower right) in the synthetic catchment

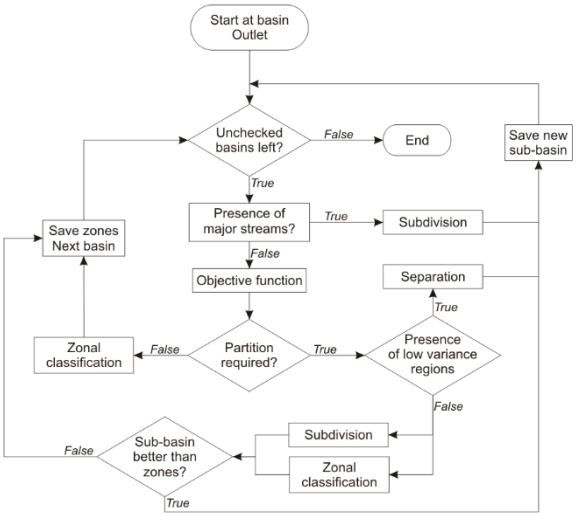

Figure 8: Sequence of the ACS-algorithm

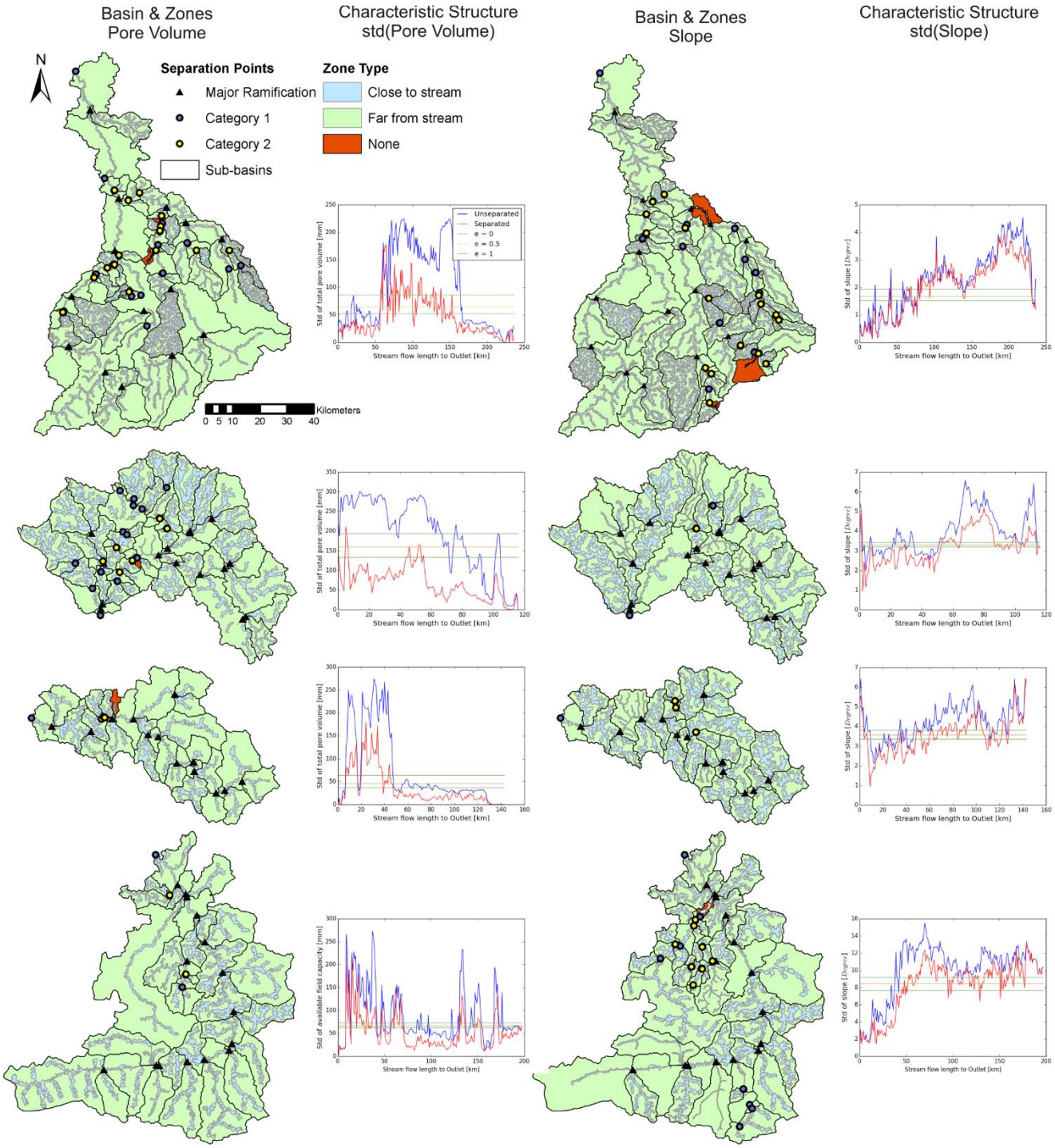

Figure 9: Results of application of *ACS* for catchments of the Mulde, Main, Regen and Salzach (from top to bottom), sub-basins based on pore volume (left) and slope (right). Comparison of σ(U) and σ(S) for each application (red and blue lines).

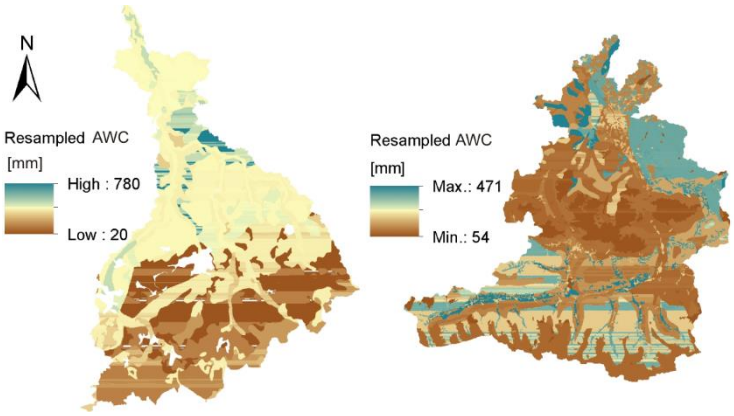

Figure 10: Resampled AWC values for Mulde and Salzach catchment (scale = 1:2500000)

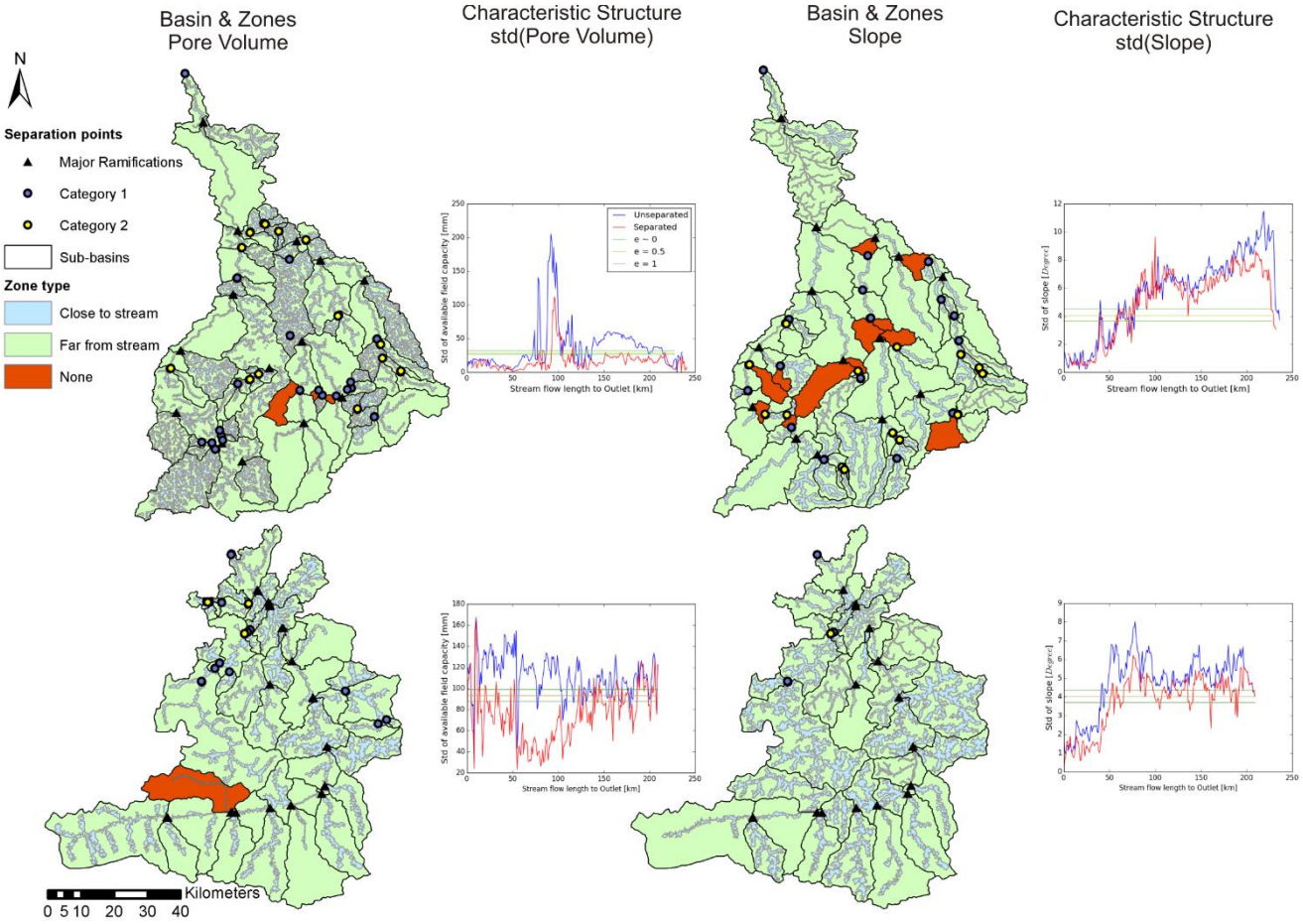

Figure 11: Results of application of the algorithm for resampled catchments of the Mulde and Salzach (from top to bottom), sub-basins based on resampled pore volume (left) and slope (right). Comparison of σ(U) and σ(S) for each application (red and blue lines).

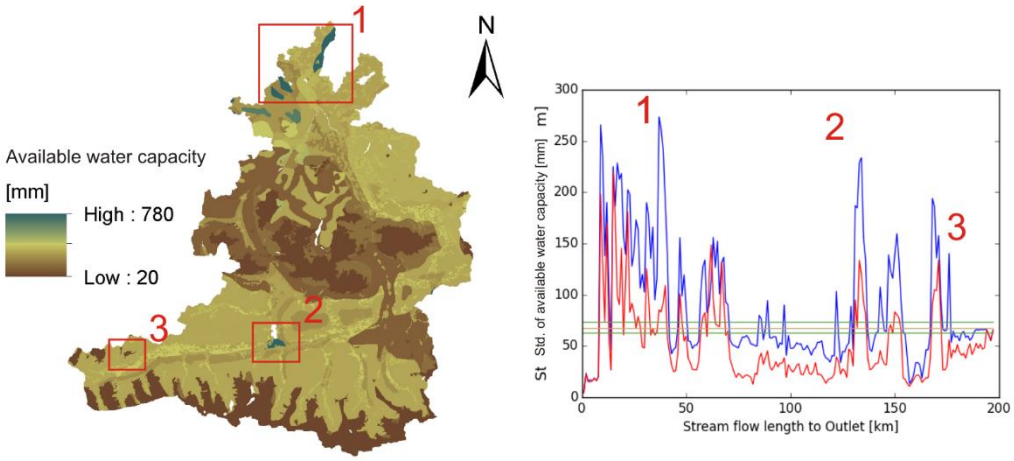

Figure 12: AWC of the Salzach catchment and the characteristic structure of σ (U) and σ (S). Red marked and numbered areas incorporating high value enclosures

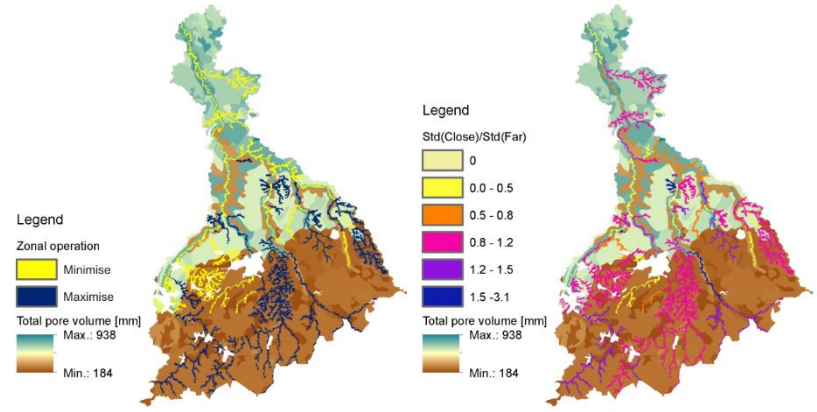

Figure 13: Operation of zonal classification (left) and proportion of σ of "close to –" and "far from stream" zones (right) in the Mulde catchment

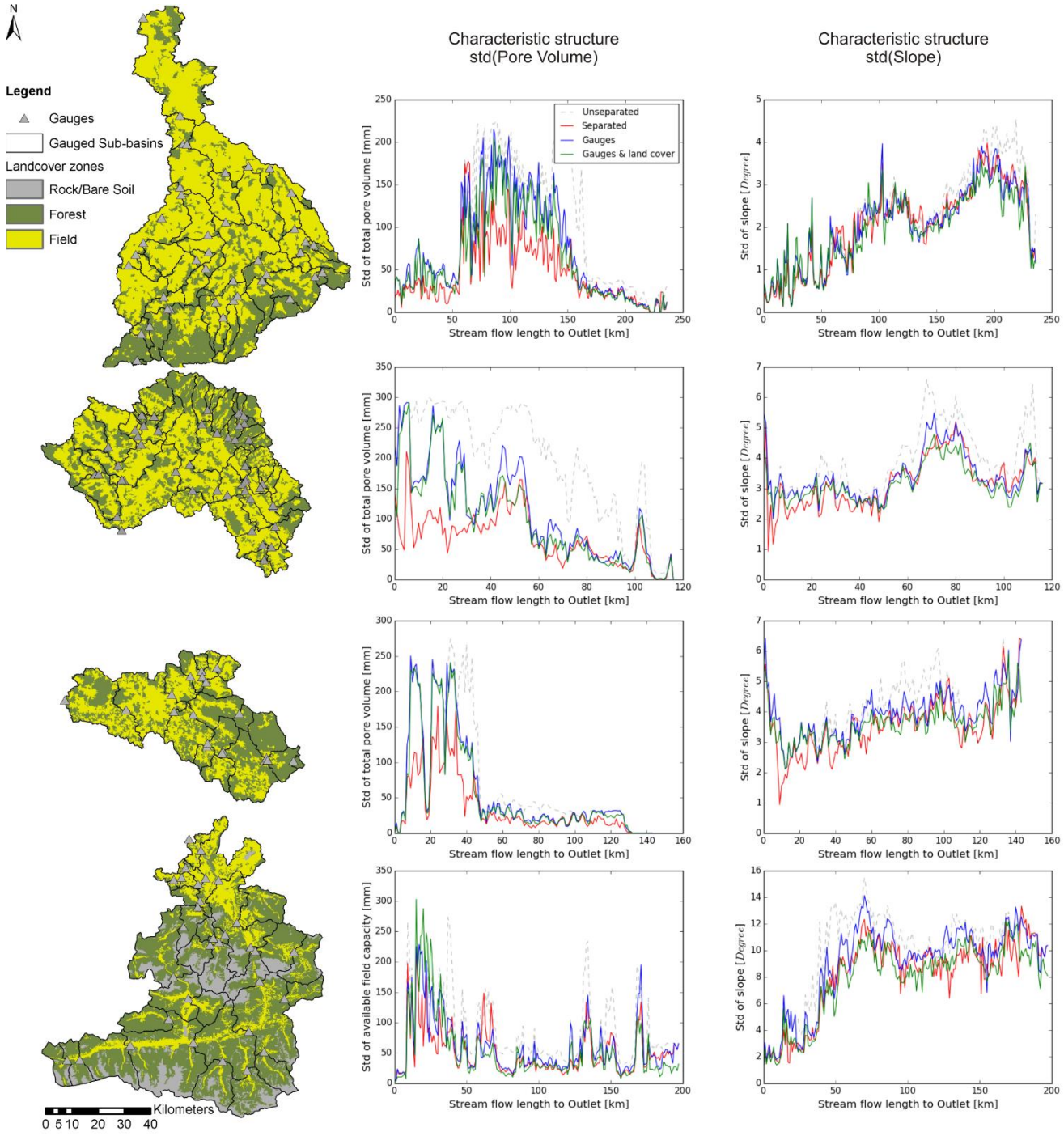

Figure 14: Subdivisions based on gauging network & zonal classification and characteristic structures of σ(pore volume) and σ(slope) (left to right) for catchments of the Mulde, Main, Regen and Salzach (top to bottom)

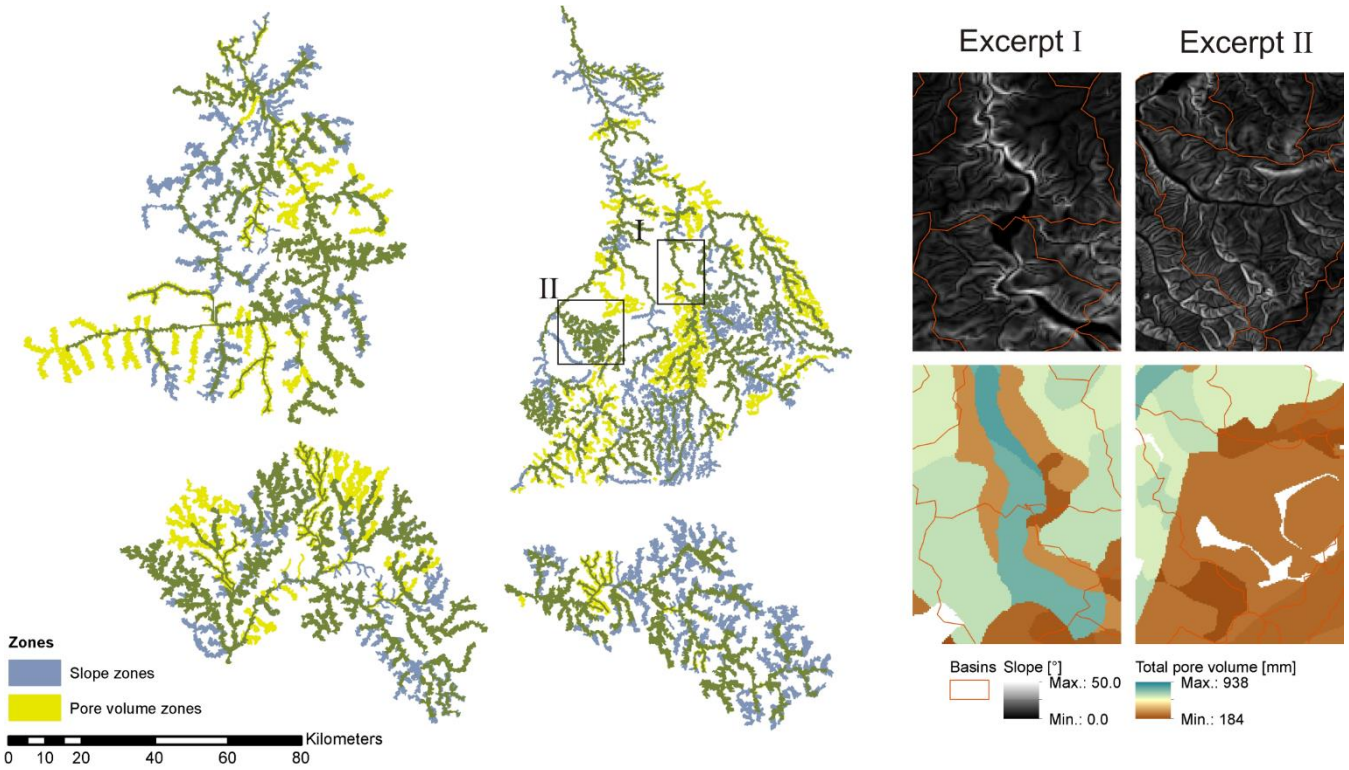

Figure 15 Left: Overlay of calculated zones for pore volume (blue) and slope (yellow), intersecting zones are shown in green. Right: Map excerpts of slope and pore volume data for indicated areas I and II

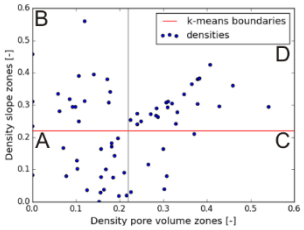

Figure 16: Scatterplot of zone densities and results of k-means cluster analysis for the Salzach catchment and assigned physiographic types (A-D)

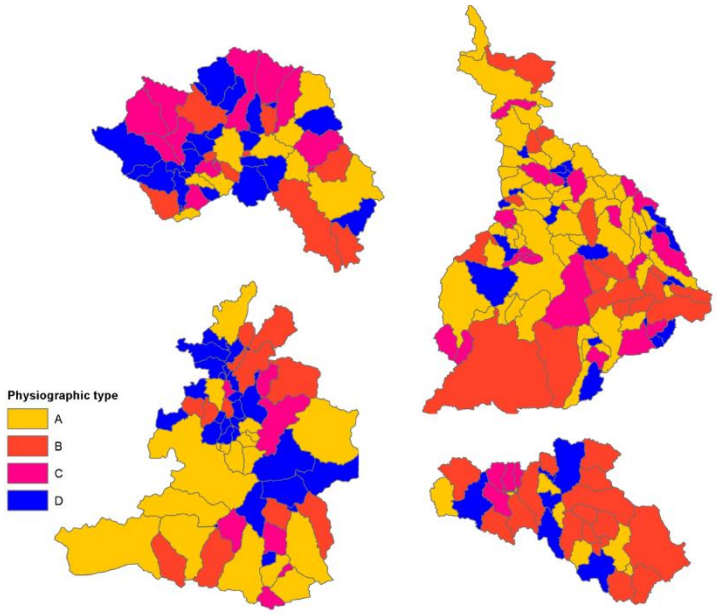

Figure 17: Identified physiographic types in case study catchments

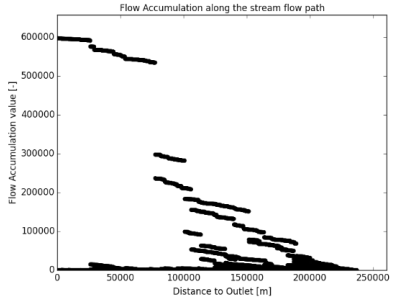

Figure A2: Characteristic structure of Flow Accumulation in the catchment of the Mulde

Figure A3: Sequence of parameter iteration for entire synthetic catchment. Iteration from upper left to lower right